

## MODELING OF SINGLE-PHASE TO THREE-PHASE DRIVE SYSTEM USING TWO PARALLEL CONVERTERS ON INPUT SIDE

G. Sudhir Kumar, G. Kumaraswamy, Dr. K. Sri Gowri

### Abstract

The objective is to supply a three phase motors from a single phase AC mains. It is common to have only a single phase power grid in residential, commercial, manufacturing and mainly in rural areas, while adjustable speed drives may require a three phase power grid. Hence we need to convert from single phase to three phase supply to operate the drive system. Parallel converters can be used to improve the power capability, reliability, efficiency and redundancy. Parallel converter techniques can be employed to improve the performance of active power filters, uninterruptable power supplies, fault tolerance of doubly fed induction generators and three phase drives. When an isolation transformer is not used, the reduction of circulating currents among different converter stages is an important objective in the system design. This work proposes a single phase to three phase drive system composed of two parallel single phase rectifiers, an induction motor and three phase inverter. The proposed system permits to reduce the rectifier switch currents, the total harmonic distortion (THD) of the grid current with same switching frequency and to increase the fault tolerance characteristics. Even with the increase in the number switches, the total energy loss of the proposed system is lower than that of conventional system. The model of the system will be derived. A suitable control strategy and pulse width modulation technique (PWM) will be developed. The complete comparison between the proposed and standard configurations will be carried out in this work. Simulation of this project will be carried out by using MATLAB/ Simulink.

**Index Terms**— Ac-dc-ac power converter, 3-phase Ac motor drive, parallel converter.

### I. INTRODUCTION

A wide variety of commercial and industrial electrical equipment requires three-phase power. Electric utilities do not install three-phase power as a matter of course because it cost significantly more than single-phase installation. Hence we need to conversion from single-phase to three-phase. Parallel converters have been used to improve the power

capability, reliability, efficiency, and redundancy. Usually the operation of converters in parallel requires a transformer for isolation. However, weight, size, and cost associated with the transformer may make such a solution undesirable [1]. When an isolation transformer is not used, the reduction of circulating currents among different converter stages is an important objective in the system design [2]–[7].

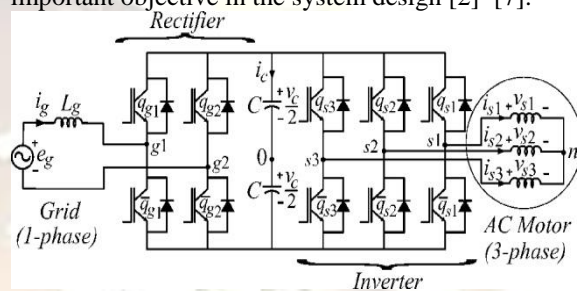


Fig. 1. Conventional single-phase to three-phase drive system.

Several solutions have been proposed when the objective is to supply three-phase motors from single-phase ac mains [8]–[16]. It is quite common to have only a single-phase power grid in residential, commercial, manufacturing, and mainly in rural areas, while the adjustable speed drives may request a three-phase power grid. Single-phase to three-phase ac–dc–ac conversion usually employs a full-bridge topology, which implies in ten power switches, as shown in Fig.1. This converter is denoted here as conventional topology. In this paper, a single-phase to three-phase drive system composed of two parallel single-phase rectifiers and a three-phase inverter is proposed, as shown in Fig. 2.

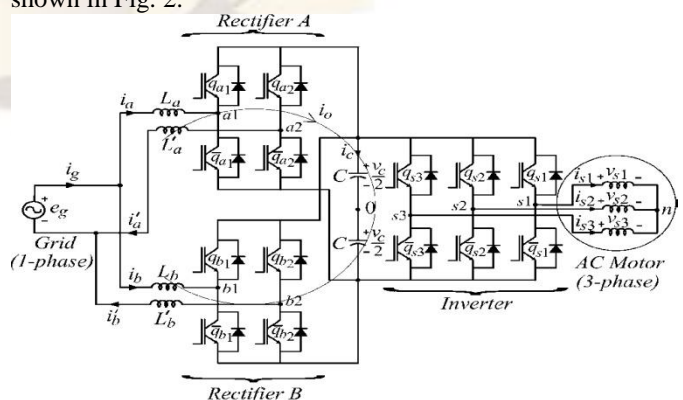


Fig.2. Proposed single-phase to three-phase drive system.

The proposed system is conceived to operate where the single-phase utility grid is the unique option available. Compared to the conventional topology, the proposed system permits: to reduce the rectifier switch currents; the total harmonic distortion (*THD*) of the grid current with same switching frequency or the switching frequency with same *THD* of the grid current; and to increase the fault tolerance characteristics. In addition, the losses of the proposed system may be lower than that of the conventional counterpart. The aforementioned benefits justify the initial investment of the proposed system, due to the increase of number of switches.

## II. PWM METHOD

Considering that  $v_a^*, v_b^*$  and  $v_o^*$  denote the reference voltages determined by the current controllers. i.e.,

$$v_a^* = v_{a10}^* - v_{a20}^* \quad (1)$$

$$v_b^* = v_{b10}^* - v_{b20}^* \quad (2)$$

$$v_o^* = v_{a10}^* + v_{a20}^* - v_{b10}^* - v_{b20}^* \quad (3)$$

The gating signals are directly calculated from the reference pole voltages  $v_{a10}^*, v_{a20}^*, v_{b10}^*$  and  $v_{b20}^*$ .

Introducing an auxiliary variable  $v_x^* = v_{a20}^*$  and solving this system of equations,

$$v_{a10}^* = v_a^* + v_x^* \quad (4)$$

$$v_{a20}^* = v_x^* \quad (5)$$

$$v_{b10}^* = (v_a^*/2) + (v_b^*/2) - (v_o^*/2) + v_x^* \quad (6)$$

$$v_{b20}^* = (v_a^*/2) - (v_b^*/2) - (v_o^*/2) + v_x^* \quad (7)$$

From these equations, it can be seen that, besides  $v_a^*, v_b^*$  and  $v_o^*$ , the pole voltages depend on also of  $v_x^*$ . The limit values of the variable  $v_x^*$  can be calculated by taking into account the maximum  $v_c^*/2$  and minimum  $-v_c^*/2$  value of the pole voltages

$$v_{x_{max}}^* = (v_c^*/2) - v_{max}^* \quad (8)$$

$$v_{x_{min}}^* = (-v_c^*/2) - v_{min}^* \quad (9)$$

Introducing a parameter  $\mu$  ( $0 \leq \mu \leq 1$ ), the variable  $v_x^*$  can be written as,

$$v_x^* = \mu v_{x_{max}}^* + (1 - \mu) v_{x_{min}}^* \quad (10)$$

Once  $v_x^*$  is chosen, pole voltages  $v_{a10}^*, v_{a20}^*, v_{b10}^*$  and  $v_{b20}^*$  are defined from (4) to (7). The parameter  $\mu$  changes the place of the voltage pulses related to  $v_a$  and  $v_b$ . And also  $\mu$  influences the harmonic distortion of the voltages generated by the rectifier.

## III. SYSTEM DESIGN

To avoid the circulating current, the following three approaches are used commonly

1) Isolation. In this approach, the overall parallel system is bulky and costly because of additional power supplies or the ac line-frequency transformer.

2) High impedance. They cannot prevent a low-frequency circulating current.

3) Synchronized control. This approach is not suitable for modular converter design. When more converters are in parallel, the system becomes very complicated to design and control.

In this proposed method the system is designed to reduce the circulating current ( $i_o$ ).

From fig.2 . the following equations can be derived for the front end rectifier

$$V_{a10} - V_{a20} = e_g - (r_a + l_a p) i_a - (r'_a + l'_a p) i'_a \quad (11)$$

$$V_{b10} - V_{b20} = e_g - (r_b + l_b p) i_b - (r'_b + l'_b p) i'_b \quad (12)$$

$$V_{a10} - V_{b10} = (r_a + l_a p) i_a - (r_b + l_b p) i_b \quad (13)$$

$$V_{a20} - V_{b20} = (r'_a + l'_a p) i'_a - (r'_b + l'_b p) i'_b \quad (14)$$

$$i_g = i_a + i_b = i'_a + i'_b \quad (15)$$

where  $p = d/dt$  and symbols like  $r$  and  $l$  represent the resistances and inductances of the input inductors. The circulating current  $i_o$  can be defined from  $i_a$  and  $i'_a$  or  $i_b$  and  $i'_b$  i.e.,

$$i_o = i_a - i'_a = -i_b + i'_b \quad (16)$$

By solving the above equations ,

$$V_a = e_g - [r_a + r'_a + (l_a + l'_a)p] i_a + (r'_a + l'_a p) i_o \quad (17)$$

$$V_b = e_g - [r_b + r'_b + (l_b + l'_b)p] i_b + (r'_b + l'_b p) i_o \quad (18)$$

$$V_o = -[r'_a + r'_b + (l'_a + l'_b)p] i_o - [r_a - r'_a + (l_a - l'_a)p] i_a + [r_b - r'_b + (l_b - l'_b)p] i_b \quad (19)$$

where

$$V_a = V_{a10} - V_{a20} \quad (20)$$

$$V_b = V_{b10} - V_{b20} \quad (21)$$

$$V_o = V_{a10} + V_{a20} - V_{b10} - V_{b20} \quad (22)$$

In order to both facilitate the control and share equally current, voltage, power between the rectifiers, the four inductors should be equal . i.e.  $r'_g = r_a = r'_a = r_b = r'_b$  and  $l'_g = l_a = l'_a = l_b = l'_b$ . In this case the model (17)-(19) can be simplified to the model given by

$$V_a + V_o/2 = e_g - 2(r'_g + l'_g p) i_a \quad (23)$$

$$V_b - V_o/2 = e_g - 2(r'_g + l'_g p) i_b \quad (24)$$

$$V_o = -2(r'_g + l'_g p) i_o \quad (25)$$

$$V_{ab} = (V_a + V_b)/2 = e_g - (r'_g + l'_g p) i_a \quad (26)$$

$$V_a - V_o/2 = e_g - 2(r'_g + l'_g p) i'_a \quad (27)$$

$$V_b + V_o/2 = e_g - 2(r'_g + l'_g p) i'_b \quad (28)$$

In this ideal case, the circulating current can be reduced to zero imposing

$$V_o = V_{a10} + V_{a20} - V_{b10} - V_{b20} = 0 \quad (29)$$

When  $i_a = 0$  then  $i_a = i'_a$  and  $i_b = i'_b$  and the system model (17)-(19) reduced to

$$V_a = e_g - 2(r'_g + l'_g p) i_a \quad (30)$$

$$V_b = e_g - 2(r'_g + l'_g p) i_b \quad (31)$$

## IV. SYSTEM CONTROL

The gating signals are obtained by comparing pole voltages with one ( $v_{r1}$ ), two ( $v_{r1}$  and  $v_{r2}$ ) or more high-frequency triangular carrier signals [17]–[20]. In the case of double-carrier approach, the phase shift of the two triangular carrier signals ( $v_{r1}$  and  $v_{r2}$ ) is  $180^\circ$ . The parameter  $\mu$  changes the place of the voltage pulses related to  $v_a$  and  $v_b$ . When  $v_x^* = v_{x_{min}}^*$  ( $\mu = 0$ ) or  $v_x^* = v_{x_{max}}^*$  ( $\mu = 1$ ) are selected, the pulses are placed in the begin or in the end of half period ( $T_s$ ) of

the triangular carrier signal.

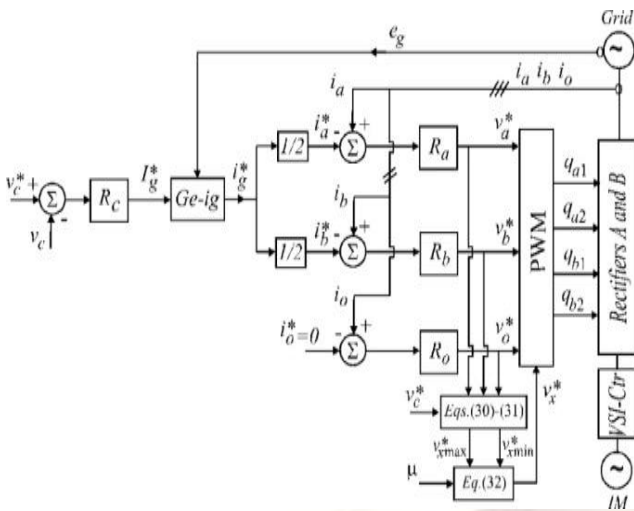


Fig. 3. Control block diagram.

The control block diagram of Fig. 2, highlighting the control of the rectifier. To control the dc-link voltage and to guarantee the grid power factor close to one. Additionally, the circulating current  $i_o$  in the rectifier of the proposed system needs to be controlled.

In this way, the dc-link voltage  $v_c$  is adjusted to its reference value  $v_c^*$  using the controller  $R_c$ , which is a standard PI type controller. This controller provides the amplitude of the reference grid current  $I_g^*$ . To control power factor and harmonics in the grid side, the instantaneous reference current  $I_g^*$  must be synchronized with voltage  $e_g$ , as given in the voltage-oriented control (VOC) for three-phase system. This is obtained via blocks  $Ge-ig$ , based on a PLL scheme. The reference currents  $i_a^*$  and  $i_b^*$  are obtained by making  $i_a^* = i_b^* = I_g^* / 2$ , which means that each rectifier receives half of the grid current. The control of the rectifier currents is implemented using the controllers indicated by blocks  $R_a$  and  $R_b$ . These current controllers define the input reference voltages  $v_a^*$  and  $v_b^*$ .

The homopolar current is measured ( $i_o$ ) and compared to its reference ( $i_o^* = 0$ ). The error is the input of PI controller  $R_o$ , that determines the voltage  $v_o^*$ . The motor three-phase voltages are supplied from the inverter (VSI). Block VSI-Ctr indicates the inverter and its control. The control system is composed of the PWM command and a torque/flux control strategy (e.g., field-oriented control or volts/hertz control).

### V. COMPARISON OF THD'S

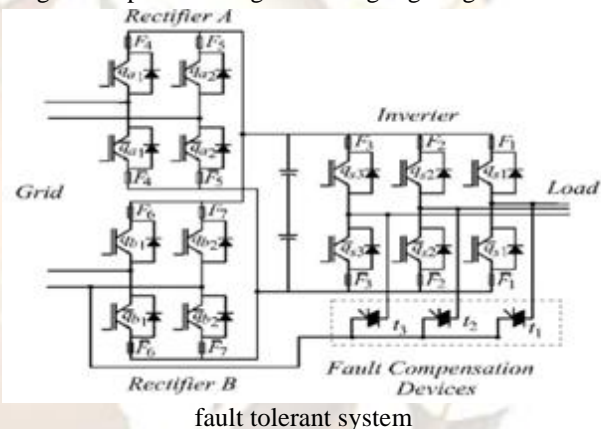
Topology (PWM)	THD <sub>p</sub> /THD <sub>c</sub>
Proposed (S-Ca $\mu = 0.5$ )	0.035
Proposed (D-Ca $\mu = 0.5$ )	0.041
Proposed (D-Ca $\mu = 0$ )	0.012

The dc-link capacitor current behavior is examined in this section. The proposed converter using double-carrier with  $\mu = 0$  provides the best reduction of the high frequency harmonics. The highest reduction of THD is obtained for the converter using double-carrier with  $\mu = 0$  and the THD obtained for  $\mu = 1$  is equal to that for  $\mu = 0$ .

By observing the above table we can say that the proposed method has lesser THD, when compared to conventional one. And also from the above table it is said that the THD of proposed one is lesser at double carrier  $\mu=0$ , when compared to single carrier  $\mu=0.5$  and double carrier  $\mu=0.5$ .

### VI. COMPENSATION OF FAULT

Fig. 4. Proposed configuration highlighting devices of



The fault compensation is achieved by reconfiguring the power converter topology with the help of isolating devices (fast active fuses— $F_j$ ,  $j = 1, \dots, 7$ ) and connecting devices (back-to-back connected SCRs— $t_1, t_2, t_3$ ), as observed in Fig. 4 and discussed in [21]–[24]. These devices are used to redefine the post-fault converter topology, which allows continuous operation of the drive after isolation of the faulty power switches in the converter. Fig. 5 presents the block diagram of the fault diagnosis system. In this figure, the block fault identification system (FIS) detects and locates the faulty switches, defining the leg to be isolated. This control system is based on the analysis of the pole voltage error.

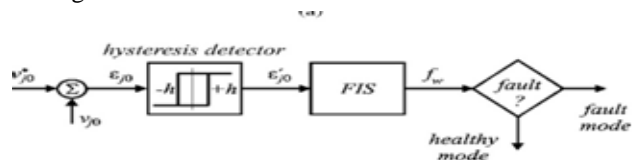


Fig.5. Block diagram of the fault diagnosis system.

The proposed system can provide compensation for open-circuit and short-circuit failures occurring in the rectifier or inverter converter devices

The fault detection and identification is carried out in four steps:

- 1) measurement of pole voltages ( $v_{j0}$ );
- 2) computation of the voltage error  $\epsilon_{j0}$  by comparison of reference voltages and measurements affected in Step 1);
- 3) determination as to whether these errors correspond or not to a faulty condition; this can be implemented by the hysteresis detector shown in Fig. 5;
- 4) Identification of the faulty switches by using  $\epsilon_{j0}$

This way, four possibilities of configurations have been considered in terms of faults:

- 1) pre-fault ("healthy") operation [see Fig. 6(a)];
- 2) post-fault operation with fault at the rectifier B [see Fig. 6(b)];
- 3) post-fault operation with fault at the rectifier A [see Fig. 6(c)];
- 4) post-fault operation with fault at the inverter [see Fig. 6(d)].

When the fault occurrence is detected and identified by the control system, the proposed system is reconfigured and becomes similar to that in Fig. 1.

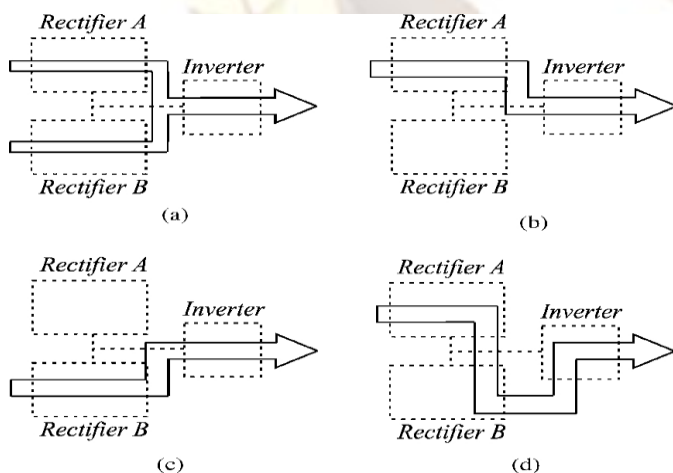


Fig. 6. Possibilities of configurations in terms of fault occurrence. (a) Pre-fault system. (b) Post-fault system with fault at the rectifier B. (c) Post-fault system with fault at the rectifier A. (d) Post-fault system with fault at the inverter.

## VII. EFFICIENCY TABLE

Frequency/Inductor	$\eta_p/\eta_c - 1$		
	S-Ca $\mu = 0.5$	D-Ca $\mu = 0.5$	D-Ca $\mu = 0$
5 kHz/ ( $L'_g = L_g$ )	-0.75 %	-0.29 %	1.61 %

By observing the above table we can conclude that the efficiency of proposed system has better at D-Ca  $\mu = 0$  as compared with the conventional system at the same operating conditions.

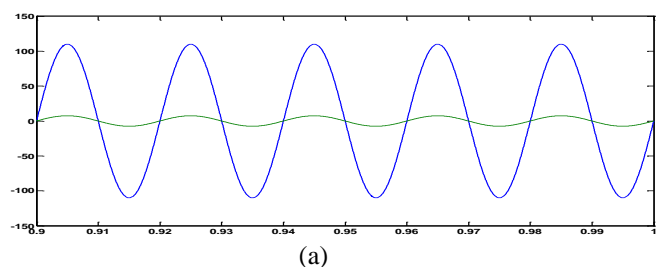
The initial investment of the proposed system is higher than that of the standard one, since the number of switches and de-vices such as fuses and triacs is highest. But, considering the scenario when faults may occur, the drive operation needs to be stopped for a nonprogrammer maintenance schedule. The cost of this schedule can be high and this justifies the high initial investment inherent of fault-tolerant motor drive systems. On the other hand, the initial investment can be justified if the *THD* of the conventional system is a critical factor.

## VIII. SIMULATION RESULTS

The steady-state simulation results are shown in Fig. 7. The waveforms in this figure are: (a) voltage and current of the grid, (b) dc-link voltage, (c) currents of rectifier A and circulating current, (d) currents of rectifiers A and B, and (e) load line voltage. Note that, with the proposed configuration, all control demanded for single-phase to three-phase converter has been established. the proposed configuration provides current reduction in the rectifier side (half of the current of the standard topology) [see Fig. 7(d)], which can provide loss reduction. Also, the control guarantees the circulating current close to zero [see Fig. 7(c)].

The same set of simulation results was obtained for transient in the machine voltages, as observed in Fig. 8

Simulation results presented in Fig. 9 show the behavior of variables of the proposed system when fault is detected in rectifier B. In this case, after fault detection given by the control system, the rectifier B has been isolated and the total flux of energy flows through rectifier A.



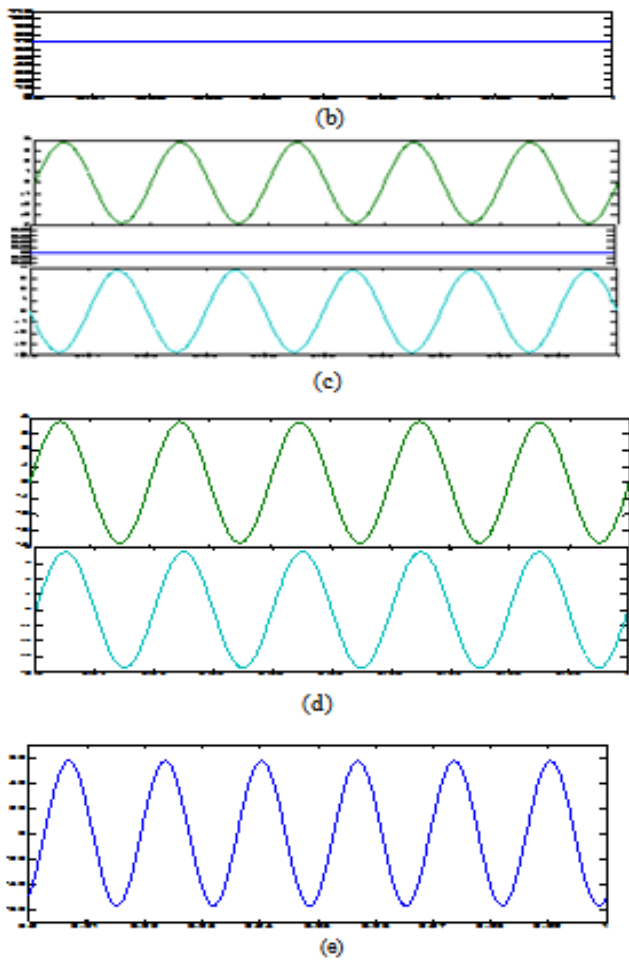


Fig. 7. Steady-state simulation results. (a) Grid voltage ( $e_g$ ) and grid current ( $i_g$ ). (b) Capacitor voltage ( $v_c$ ). (c) Currents of rectifier A ( $i_a$  and  $i_a^*$ ) and circulating current ( $i_o$ ). (d) Currents of rectifiers A ( $i_a$ ) and B ( $i_b$ ). (e) Line voltage of the load ( $v_{s 2 3}$ ).

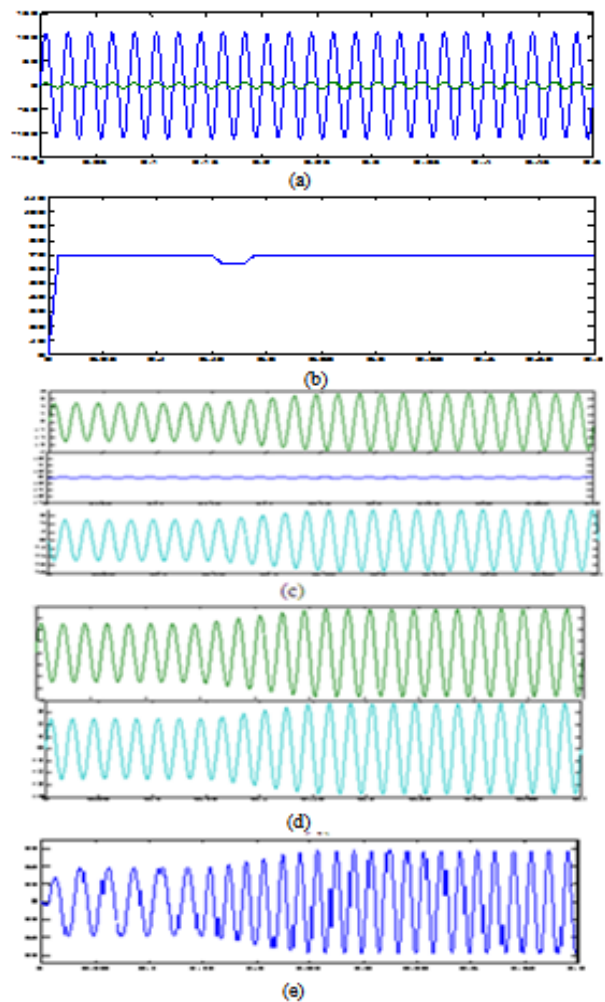
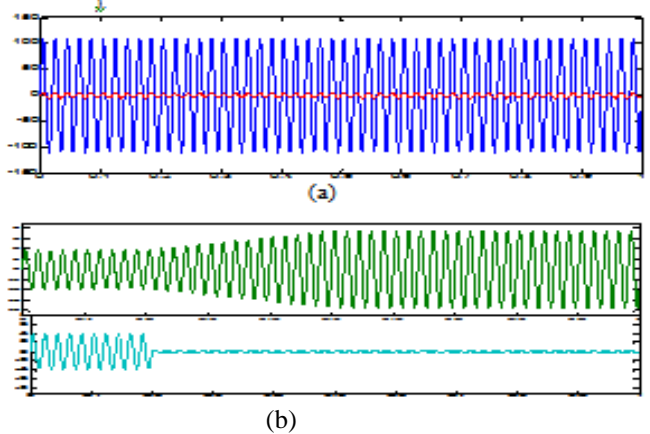


Fig. 8. Simulation results for a volts/hertz transient applied to the three-phase motor. (a) Grid voltage ( $e_g$ ) and grid current ( $i_g$ ). (b) Capacitor volt-age ( $v_c$ ). (c) Currents of rectifier A ( $i_a$  and  $i_a^*$ ) and circulating current ( $i_o$ ). (d) Currents of rectifiers A ( $i_a$ ) and B ( $i_b$ ). (e) Line voltage of the load ( $v_{s 2 3}$ ).



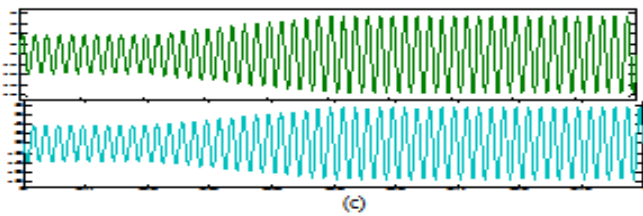


Fig. 9. Simulation results of the proposed configuration when a fault is identified at the rectifier B. (a) Grid voltage ( $e_g$ ) and grid current ( $i_g$ ). (b) Currents of rectifiers A ( $i_a$ ) and B ( $i_b$ ). (c) Currents of rectifier A ( $i_a$  and  $i_a^*$ ).

## IX. CONCLUSION

The system combines two parallel rectifiers without the use of transformers. The system model and the control strategy, including the PWM technique, have been developed.

The complete comparison between the proposed and standard configurations has been carried out in this work. Compared to the conventional topology, the proposed system permits to reduce the rectifier switch currents, the THD of the grid current and to increase the fault tolerance characteristics.

The simulation results have shown that the system is controlled properly, even with transient and occurrence of faults

## REFERENCES

- [1] J.-K. Park, J.-M. Kwon, E.-H. Kim, and B.-H. Kwon, "High-performance transformerless online UPS," *IEEE Trans. Ind. Electron.*, vol. 55, no. 8, pp. 2943–2953, Aug. 2008.
- [2] Z. Ye, D. Boroyevich, J.-Y. Choi, and F. C. Lee, "Control of circulating current in two parallel three-phase boost rectifiers," *IEEE Trans. Power Electron.*, vol. 17, no. 5, pp. 609–615, Sep. 2002.
- [3] S. K. Mazumder, "Continuous and discrete variable-structure controls for parallel three-phase boost rectifier," *IEEE Trans. Ind. Electron.*, vol. 52, no. 2, pp. 340–354, Apr. 2005.
- [4] X. Sun, L.-K. Wong, Y.-S. Lee, and D. Xu, "Design and analysis of an optimal controller for parallel multi-inverter systems," *IEEE Trans. Circuits Syst. II*, vol. 53, no. 1, pp. 56–61, Jan. 2006.
- [5] Z. Ye, P. Jain, and P. Sen, "Circulating current minimization in high-frequency AC power distribution architecture with multiple inverter modules operated in parallel," *IEEE Trans. Ind. Electron.*, vol. 54, no. 5, pp. 2673–2687, Oct. 2007.
- [6] P.-T. Cheng, C.-C. Hou, and J.-S. Li, "Design of an auxiliary converter for the diode rectifier and the analysis of the circulating current," *IEEE Trans. Power Electron.*, vol. 23, no. 4, pp. 1658–1667, Jul. 2008.
- [7] H. Cai, R. Zhao, and H. Yang, "Study on ideal operation status of parallel inverters," *IEEE Trans. Power Electron.*, vol. 23, no. 6, pp. 2964–2969, Nov. 2008.
- [8] P. Enjeti and A. Rahman, "A new single phase to three phase converter with active input current shaping for low cost AC motor drives," *IEEE Trans. Ind. Appl.*, vol. 29, no. 2, pp. 806–813, Jul./Aug. 1993.
- [9] J. Itoh and K. Fujita, "Novel unity power factor circuits using zero-vector control for single-phase input systems," *IEEE Trans. Power Electron.*, vol. 15, no. 1, pp. 36–43, Jan. 2000.
- [10] B. K. Lee, B. Fahimi, and M. Ehsani, "Overview of reduced parts converter topologies for AC motor drives," in *Proc. IEEE PESC*, 2001, pp. 2019–2024.
- [11] C. B. Jacobina, M. B. de R. Correa, A. M. N. Lima, and E. R. C. da Silva, "AC motor drive systems with a reduced switch count converter," *IEEE Trans. Ind. Appl.*, vol. 39, no. 5, pp. 1333–1342, Sep./Oct. 2003.
- [12] R. Q. Machado, S. Buso, and J. A. Pomilio, "A line-interactive single-phase to three-phase converter system," *IEEE Trans. Power Electron.*, vol. 21, no. 6, pp. 1628–1636, May 2006.
- [13] O. Ojo, W. Zhiqiao, G. Dong, and S. Asuri, "High-performance speed-sensorless control of an induction motor drive using a minimalist single-phase PWM converter," *IEEE Trans. Ind. Appl.*, vol. 41, no. 4, pp. 996–1004, Jul./Aug. 2005.
- [14] J. R. Rodríguez, J. W. Dixon, J. R. Espinoza, J. Pontt, and P. Lezana, "PWM regenerative rectifiers: State of the art," *IEEE Trans. Ind. Electron.*, vol. 52, no. 1, pp. 5–22, Feb. 2005.
- [15] M. N. Uddin, T. S. Radwan, and M. A. Rahman, "Fuzzy-logic-controller-based cost-effective four-switch three-phase inverter-fed IPM synchronous motor drive system," *IEEE Trans. Ind. Appl.*, vol. 42, no. 1, pp. 21–30, Jan./Feb. 2006.
- [16] D.-C. Lee and Y.-S. Kim, "Control of single-phase-to-three-phase AC/DC/AC PWM converters for induction motor drives," *IEEE Trans. Ind. Electron.*, vol. 54, no. 2, pp. 797–804, Apr. 2007.
- [17] J. Holtz, "Pulsewidth modulation for electronic power conversion," *Proc. IEEE*, vol. 82, no. 8, pp. 1194–1214, Aug. 1994.
- [18] A. M. Trzynadlowski, R. L. Kirlin, and S. F. Legowski, "Space vector PWM technique with minimum switching losses and a variable pulse

- rate,” *IEEE Trans. Ind. Electron.*, vol. 44, no. 2, pp. 173–181, Apr. 1997.
- [19] O. Ojo and P. M. Kshirsagar, “Concise modulation strategies for four-leg voltage source inverters,” *IEEE Trans. Power Electron.*, vol. 19, no. 1, 46–53, Jan. 2004.
- [20] C. B. Jacobina, A. M. N. Lima, E. R. C. da Silva, R. N. C. Alves, and P. F. Seixas, “Digital scalar pulse-width modulation: a simple approach to introduce non-sinusoidal modulating waveforms,” *IEEE Trans. Power Electron.*, vol. 16, no. 3, pp. 351–359, May 2001.
- [21] R. L. A. Ribeiro, C. B. Jacobina, E. R. C. da Silva, and A. M. N. Lima, “Fault detection of open-switch damage in voltage-fed PWM motor drive systems,” *IEEE Trans. Power Electron.*, vol. 18, no. 2, pp. 587–593, Apr. 2003.
- [22] B. A. Welchko, T. A. Lipo, T. M. Jahns, and S. E. Schulz, “Fault tolerant three-phase AC motor drive topologies: A comparison of features, cost, and limitations,” *IEEE Trans. Power Electron.*, vol. 19, no. 4, pp. 1108–1116, Jul. 2004.
- [23] S. Kwak and H. Toliyat, “An approach to fault-tolerant three-phase matrix converter drives,” *IEEE Trans. Energy Convers.*, vol. 22, no. 4, pp. 855–863, Dec. 2003.
- [24] D. Campos-Delgado, D. Espinoza-Trejo, and E. Palacios, “Fault-tolerant control in variable speed drives: A survey,” *IET Electr. Power Appl.*, vol. 2, no. 2, pp. 121–134, Mar. 2008.

Pradesh, India. He has eight years of teaching experience. He has attended several National workshops. His main areas of research include Photovoltaic cells, Multilevel inverters. Email:kumar1718@gmail.com



**Dr. K.Sri Gowri** received the B.Tech degree from SVU college of Engineering, Tirupati in 1997, the M.Tech degree from RGM College of Engineering and Technology, Nandyal and has been awarded Ph.D in the area of Power Electronic Control of Electric Drives from JNTU Kakinada in 2010. She is currently Professor in the Department of EEE in RGM CET, Nandyal, A.P. Her areas of interest include Power Electronics, Pulse Width Modulation Techniques, Drives and Control, Renewable Sources of Energy. E-mail: gowrivasu.3@gmail.com

## BIOGRAPHIES



**G.sudhir kumar** is born in 1990 in India .He is graduated from JNTU Anantapur in 2011.Presently he is doing post graduation in Power Electronics and Electrical drives Specialization at J.N.T.U.A. Anantapur. His main areas of interest include Induction motor drives, Electrical machines, power Electronic converters and Power Electronic Drives



**G. Kumaraswamy** is born in 1983 in India. He is graduated from JNTU University in 2005 and pursued Post graduation from the same university. He is currently working as a Assistant professor in the department of electrical and electronics engineering R.G.M college of engineering and technology, Nandyal, Andhra